

# $^1\text{H}$ Chemical Shielding Anisotropies from Polycrystalline Powders Using MSHOT-3 Based CRAMPS

M. Hohwy, J. T. Rasmussen, P. V. Bower, H. J. Jakobsen, and N. C. Nielsen

*Instrument Centre for Solid-State NMR Spectroscopy, Department of Chemistry, University of Aarhus, DK-8000 Aarhus C, Denmark*

Received August 29, 1997; revised December 2, 1997

**It is demonstrated that combined rotation and multiple-pulse spectroscopy (CRAMPS) based on MSHOT-3 homonuclear multiple-pulse decoupling represents a powerful method for determination of  $^1\text{H}$  chemical shielding anisotropies from polycrystalline powders. By virtue of high-order dipolar decoupling, large spectral width, resonance offset stability, and the absence of artifacts from tilted-axis precession, MSHOT-3-based CRAMPS enables straightforward sampling of high-quality spectra. Comparison with explicit calculations, taking the effect of the multiple-pulse sequence into account, shows that the spectra may be simulated and iteratively fitted using standard software for the calculation of magic-angle spinning spectra influenced by chemical shielding anisotropy with the shielding interaction reduced by the scaling factor of the MSHOT-3 decoupling sequence. The method is demonstrated by experimental determination of  $^1\text{H}$  chemical shielding anisotropies for adipic acid,  $\text{Ca}(\text{OH})_2$ , malonic acid, and  $\text{KHSO}_4$ . The data are compared with those determined previously from single-crystal NMR studies.** © 1998 Academic Press

Over the years anisotropic nuclear spin interactions have confronted the solid-state NMR spectroscopist with large technological challenges as compared to NMR studies in the isotropic phase. However, when handled appropriately these interactions represent an important source of information regarding molecular structure and dynamics in the solid state. For example, dipolar interactions provide information about internuclear distances and spin–spin coupling networks, while the chemical shielding and quadrupolar coupling interactions probe the local electronic environment of the nucleus. Focusing on the chemical shielding interaction, tensor values may be determined using single-crystal, static-powder, or magic-angle spinning (MAS) NMR (1–3). In particular, for nonabundant spin-1/2 nuclei the principal components of the chemical shielding tensor have been obtained in a straightforward manner using standard MAS NMR.

For abundant spins, such as  $^1\text{H}$ ,  $^{19}\text{F}$ , and  $^{31}\text{P}$ , homogeneous interactions (4) from homonuclear dipolar couplings may severely hamper a direct determination of the shielding tensor components by MAS NMR. In this case, it is necessary to consider all active interactions (which in general is complicated and therefore is restricted to small spin systems) or to use

homonuclear multiple-pulse decoupling (5–9) for averaging the homonuclear dipolar interactions. While the latter method, usually referred to as combined rotation and multiple-pulse spectroscopy (CRAMPS) (10–13), has become well established for measuring the isotropic part of  $^1\text{H}$ ,  $^{19}\text{F}$ , and  $^{31}\text{P}$  chemical shielding tensors (14–18), only very few studies have considered its use for measuring chemical shielding anisotropies (CSAs) under MAS (15, 16) and off-MAS (19) conditions. This may be ascribed to the fact that CRAMPS typically faces one or more of the well-known problems: (i) low spectral width caused by the long cycle times typical for high-order decoupling sequences, (ii) instability toward resonance off-sets, (iii) artifacts from tilted-axis precession, or (iv) insufficient decoupling performance. To remedy the first two problems previous attempts to determine  $^{19}\text{F}$  and  $^{31}\text{P}$  CSAs (15, 16) used MREV-8-based (6, 7) CRAMPS which, however, suffers from one or both of the two latter problems. For determination of  $^1\text{H}$  CSAs, the need for efficient and artifact-free decoupling is particularly important because of the strong homonuclear dipolar interactions and the low dispersion in isotropic chemical shifts. In this Communication, we demonstrate that these problems may largely be solved using CRAMPS based on the high-order truncating MSHOT-3 homonuclear decoupling sequence (20, 21) shown schematically in Fig. 1. Using this method, we show what to our knowledge represents the first accurate measurements of  $^1\text{H}$  CSAs from homonuclear decoupled MAS spectra of polycrystalline powders.

Figure 2a shows a 400-MHz  $^1\text{H}$  CRAMPS spectrum for adipic acid obtained using MSHOT-3 multiple-pulse decoupling. The spectrum was recorded on a Varian UNITY-400 spectrometer using a multipurpose probe from Doty Scientific, Inc., with a 5-mm  $\text{Si}_3\text{N}_4$  rotor (spherical sample chamber of Kel-F, 2 mm i.d.) and using a MAS frequency  $\omega_r/2\pi = 584$  Hz and a nominal radiofrequency (RF) field strength  $\omega_{\text{RF}}/2\pi = 119$  kHz. Taking into account the effects from finite pulse rise times and from small delays (see the caption of Fig. 2) for quadrature phase setting (cf. Fig. 1), this corresponds to rotor synchronization with 18 MSHOT-3 cycles per rotor period ( $N = 18$ ). With the chemical shift terms scaled by a factor 0.352 (measured experimentally) using MSHOT-3, sampling prior to each MSHOT-3 cycle leads to a spectral width of 42

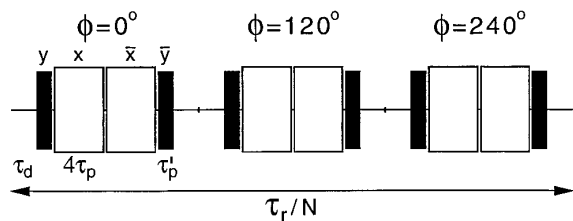


**FIG. 1.** Timing scheme of the MSHOT-3 homonuclear decoupling sequence (20) employed for the determination of magnitudes of  $^1\text{H}$  chemical shielding tensors using CRAMPS. The effective amplitude of the bracketing ( $(\pi/2)_{\pm y}$  (filled bars) and the  $(2\pi)_{\pm x}$  (open bars) pulses are different (corresponding to effective  $90^\circ$  pulses of duration  $\tau_p'$  and  $\tau_p$ , respectively) to mimic the effect of finite pulse rise times.  $\tau_d = 2\tau_p - \tau_p'/4$  and  $\phi$  represent the bracketing delay and the overall phase (in addition to the quadrature phases  $y$ ,  $x$ ,  $\bar{x}$ ,  $\bar{y}$ ) of the three magic sandwich elements (22) constituting the MSHOT-3 sequence, respectively. Furthermore, a small delay (see the caption of Fig. 2) is inserted between adjacent RF pulses to allow accurate quadrature phase setting. The pulse sequence is rotor synchronized to an integral number  $N$  (larger than 3 (21)) of MSHOT-3 cycles within the rotor period  $\tau_r = 2\pi/\omega_r$  and one complex data point is sampled prior to each MSHOT-3 cycle.

ppm, clearly sufficient to accommodate the full spinning sideband patterns from the three different proton resonances for adipic acid. A deconvoluted spectrum (Fig. 2b) is shown below the experimental spectrum. The sideband manifold from the carboxylic proton resonance has been deconvoluted using a pure Lorentzian lineshape which indicates efficient truncation of the dipolar interaction. In contrast, a Gaussian contribution to the lineshape is required for deconvolution of the spinning sidebands from the  $\text{CH}_2$  protons, which suggests influence from residual dipolar couplings.

Based on the deconvolution, it is possible to separate the three overlapping spinning sideband manifolds for the carboxylic and methylene protons in order to obtain reliable spinning sideband intensities for iterative fitting. As an example, Fig. 2c shows the deconvoluted  $^1\text{H}$  CRAMPS spectrum of the carboxylic protons which may be iteratively fitted to give the simulated sideband spectrum in Fig. 2d and the chemical shielding parameters in Table 1. Within a first approximation, these calculations are based solely on the anisotropic chemical shielding interaction scaled by the factor 0.352 of MSHOT-3 decoupling (i.e., the pulse sequence is not considered explicitly). The excellent agreement between experimental and calculated spectra immediately indicates that this assumption is acceptable in practice.

To investigate the validity of the approximation, ignoring the multiple-pulse irradiation in the calculation of  $^1\text{H}$  CRAMPS spectra, we conducted a series of simulations explicitly taking into account the MSHOT-3 RF irradiation. These simulations have been compared with spectra calculated within the simple scaling approach described above. Figure 3 shows two representative sets of  $^1\text{H}$  CRAMPS spectra calculated using the tensor values for the carboxylic protons of adipic acid (Table 1) and different spinning frequencies within the regime relevant for determination of  $^1\text{H}$  CSAs at a Larmor frequency of 400 MHz. The spectra corre-

sponding to  $\omega_r/2\pi = 584$  Hz (Figs. 3a and 3b) and 1051 Hz (Figs. 3c and 3d) are calculated using the pulse sequence in Fig. 1 rotor-synchronized to accommodate 18 and 10 MSHOT-3 cycles within the rotor period, respectively. To closely match the experimental conditions, the explicit MSHOT-3 calculations (Figs. 3a and 3c) considered effects from finite pulse rise times and delays for accurate quadrature phase setting as described in the caption of Fig. 2. The very close agreement between the simulations in Fig. 3 taking the MSHOT-3 RF irradiation into account (Figs. 3a and 3c) and just assuming a 0.352 scaling of the chemical shielding interaction (Figs. 3b and 3d) clearly demonstrates that the approximation of a locally time-independent Hamiltonian (i.e., the simple scaling approach) is acceptable in experimentally relevant cases concerning the determination of  $^1\text{H}$  CSAs. This conclusion

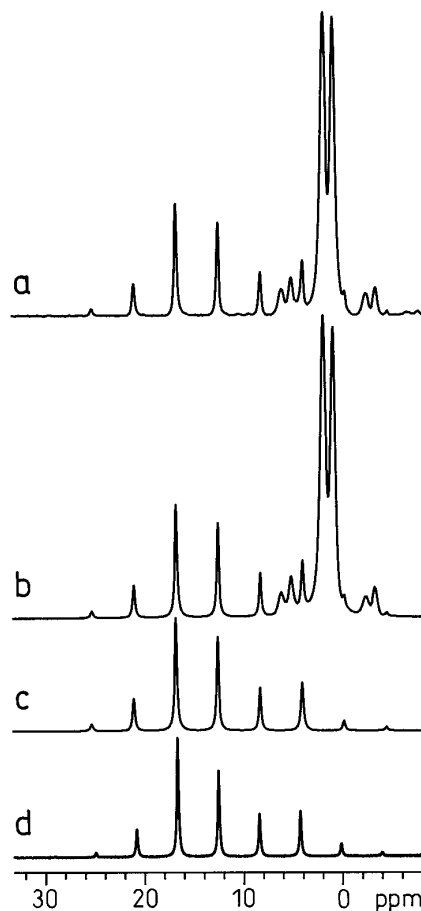


**FIG. 2.**  $^1\text{H}$  CRAMPS (400 MHz) spectra of adipic acid recorded using MSHOT-3 multiple-pulse decoupling. (a) Experimental spectrum recorded using the pulse sequence in Fig. 1 with  $\omega_r/2\pi = 584$  Hz,  $N = 18$ ,  $\tau_p = 2.2$   $\mu\text{s}$  (effective  $\omega_{\text{RF}}/2\pi = 119$  kHz),  $\tau_p' = 2.55$   $\mu\text{s}$  (effective  $\omega_{\text{RF}}/2\pi = 98$  kHz), a 0.6- $\mu\text{s}$  delay between adjacent pulses to allow optimum quadrature phase setting, 128-s relaxation delay, and 64 scans. (b) Deconvoluted spectrum using Lorentzian (carboxylic protons) and Lorentzian/Gaussian lineshapes (methylene protons). (c) Deconvoluted spectrum for the carboxylic protons only. (d) Simulated  $^1\text{H}$  spectrum resulting from iterative fitting of the spectrum in (c). In the calculations the effect of MSHOT-3 decoupling is taken into account solely by scaling of the chemical shielding terms by 0.352.

**TABLE 1**  
 $^1\text{H}$  Chemical Shielding Parameters Determined by Iterative Fitting of Spinning Sideband Intensities from MSHOT-3-Based CRAMPS Spectra<sup>a</sup>

Compound	$\sigma_{\text{iso}}$ (ppm)	$\sigma_{\text{aniso}}$ (ppm)	$\eta$	Ref.
Adipic acid (–OH)	–12.6 (–13.6)	–13.1	0.25	(23)
Ca(OH) <sub>2</sub>	–1.1 (–4.6)	–9.6 (–9.3)	0.00 (0.0)	(24)
Malonic acid (–OH, site 1)	–12.5 (–12.6)	–12.4 (–12.8)	0.39 (0.40)	(25)
Malonic acid (–OH, site 2)	–12.1 (–11.9)	–12.6 (–12.6)	0.20 (0.35)	(25)
KHSO <sub>4</sub> (site 1)	–10.8 (–12.6)	–16.6 (–16.2)	0.16 (0.06)	(1)
KHSO <sub>4</sub> (site 2)	–12.1 (–14.4)	–18.3 (–18.0)	0.45 (0.09)	(1)

<sup>a</sup> Relative to external TMS. Estimated absolute uncertainties of  $\pm 0.2$  ppm for  $\sigma_{\text{iso}}$ ,  $\sigma_{\text{aniso}}$  and  $\pm 0.1$  for  $\eta$ . Numbers in parentheses correspond to the reference indicated in the right column. The chemical shielding parameters used the definitions  $\sigma_{\text{iso}} = (\sigma_{xx} + \sigma_{yy} + \sigma_{zz})/3$ ,  $\sigma_{\text{aniso}} = \sigma_{zz} - \sigma_{\text{iso}}$ , and  $\eta = (\sigma_{yy} - \sigma_{xx})/\sigma_{\text{aniso}}$  using the ordering  $|\sigma_{zz} - \sigma_{\text{iso}}| \geq |\sigma_{xx} - \sigma_{\text{iso}}| \geq |\sigma_{yy} - \sigma_{\text{iso}}|$ .

is of considerable practical importance since it implies that spectral analysis can be restricted to the use of standard software solely taking into account the scaled chemical shielding interaction under MAS conditions.

Because of significant residual homonuclear dipolar couplings (manifested by broad, partly Gaussian lineshapes) and small CSAs we did not attempt assessment of  $\sigma_{\text{aniso}}$  and  $\eta$  for the methylene protons of adipic acid under the present experimental conditions (Fig. 2). However, since the most important residual coupling term for MSHOT-3 decoupling is of third order and scales inversely proportional to the second power of the RF field strength (20, 21), sufficient decoupling may be achieved by increasing the RF field strength. To explore the capability of the method using state-of-the-art RF field strengths, Fig. 4 shows numerical MSHOT-3 CRAMPS spectra

for a  $^1\text{H}$ – $^1\text{H}$  spin pair with parameters typical for geminal coupled methylene protons (see figure caption for details). The spectrum in Fig. 4a corresponds to decoupling with the moderate RF fields used experimentally in this work which clearly

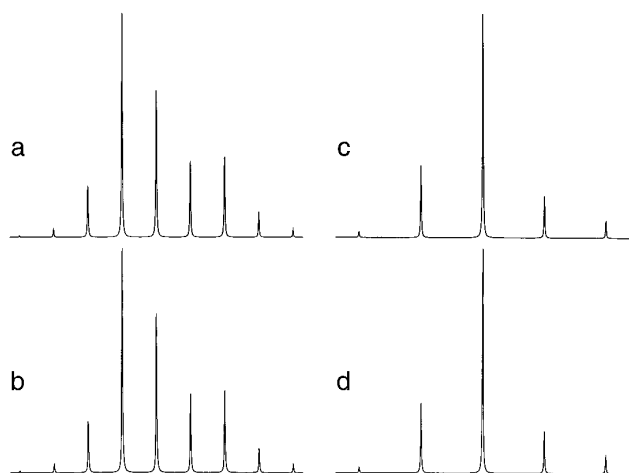


**FIG. 3.** Calculated  $^1\text{H}$  CRAMPS spectra using the chemical shielding parameters for the carboxylic protons in adipic acid and (a, b)  $\omega_r/2\pi = 584$  Hz ( $N = 18$ ) and (c, d)  $\omega_r/2\pi = 1051$  Hz ( $N = 10$ ). The spectra in (a, c) were calculated by taking explicitly into account the MSHOT-3 multiple-pulse sequence in Fig. 1 (see text), while those in (b, d) were calculated considering only the chemical shielding interaction being scaled by the experimentally determined factor of 0.352.

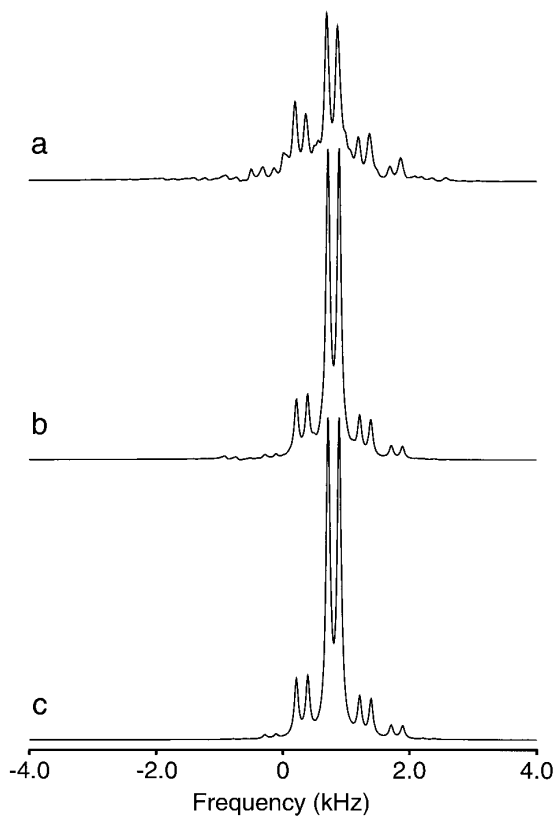


**FIG. 4.** Numerical  $^1\text{H}$  CRAMPS (400 MHz) spectra for a homonuclear  $^1\text{H}$ – $^1\text{H}$  spin-pair system undergoing MSHOT-3 CRAMPS. The two spins (A and B) are characterized by  $\sigma_{\text{iso}}^{\text{A}} = -3.75$  ppm,  $\sigma_{\text{iso}}^{\text{B}} = -5$  ppm,  $\sigma_{\text{aniso}}^{\text{A}} = \sigma_{\text{aniso}}^{\text{B}} = -5$  ppm,  $\eta_{\text{A}} = \eta_{\text{B}} = 0$ , angles  $35^\circ$  and  $-35^\circ$  distinguishing the most shielded tensor axes from the internuclear axis, and a dipolar coupling constant of  $b_{\text{AB}}/2\pi = 22$  kHz (a, b) and 0 (c). The experimental parameters are as in Fig. 1 in (a), while the RF field strength was increased to  $\omega_{\text{RF}}/2\pi = 300$  kHz ( $\tau_{\text{p}} = \tau_{\text{p}}^* = 0.83$   $\mu\text{s}$ ,  $\tau_{\text{c}} = 33.75$   $\mu\text{s}$ ) in (b) and (c).

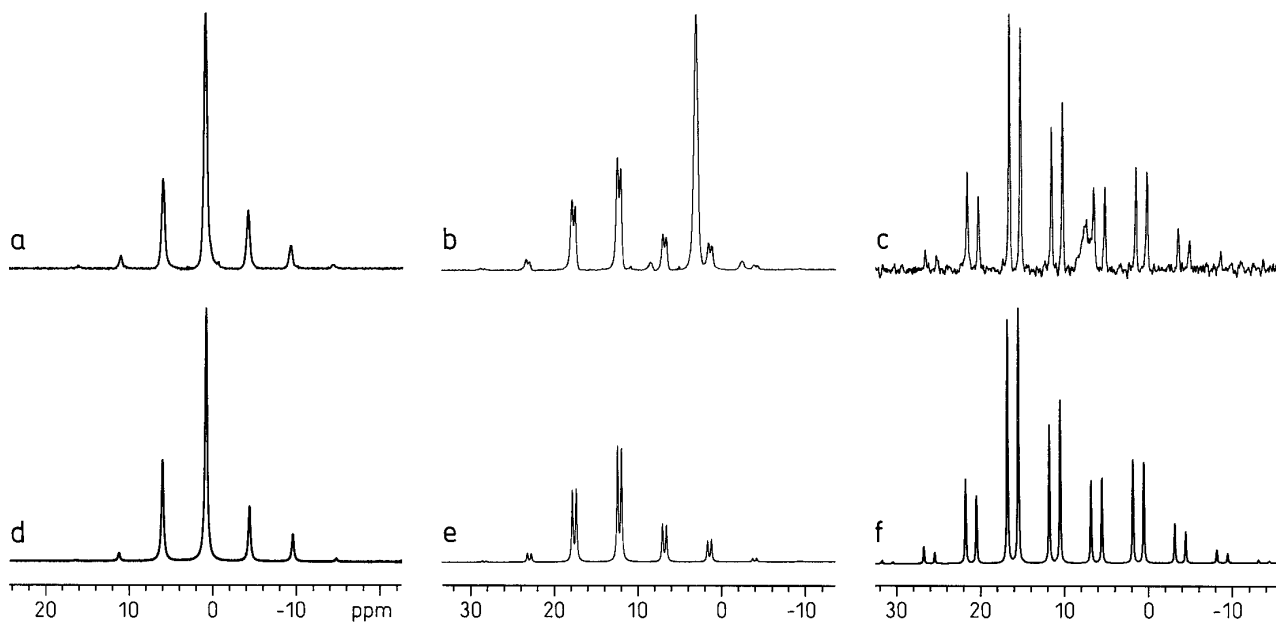


**FIG. 5.**  $^1\text{H}$  CRAMPS (400 MHz) spectra of (a, d)  $\text{Ca}(\text{OH})_2$  ( $\omega_r/2\pi = 710$  Hz,  $N = 15$ , 16-s relaxation delay, 128 scans), (b, e) malonic acid ( $\omega_r/2\pi = 751$  Hz,  $N = 14$ , 128-s relaxation delay, 16 scans), and (c, f)  $\text{KHSO}_4$  ( $\omega_r/2\pi = 697$  Hz,  $N = 15$ , 128-s relaxation delay, 16 scans; the low sensitivity in the experimental spectrum is ascribed to extremely long  $T_1$  values). (a–c) Experimental spectra. (d–f) Simulations obtained by iterative fitting of the experimental spectra in (a–c) and corresponding to the chemical shielding parameters in Table 1. The effect of MSHOT-3 decoupling was taken into consideration by scaling the chemical shift terms by a factor of 0.352.

provide insufficient decoupling. By increasing the RF field strength to 300 kHz, achievable using dedicated CRAMPS probes, the influence from residual dipolar coupling is reduced to a controllable level as demonstrated by the spectrum in Fig. 4b. By comparison with the same simulation using a dipolar coupling of zero (Fig. 4c), it is apparent that high RF field decoupling may enable extraction of reliable CSA parameters from the intensities of the spinning sideband pattern. Attempts to determine the CSA parameters from the spectrum in Fig. 4a would lead to a gross overestimation of the shielding anisotropy.

To demonstrate the general applicability of MSHOT-3 based CRAMPS for the determination of magnitudes for  $^1\text{H}$  chemical shielding tensors, Fig. 5 shows experimental  $^1\text{H}$  CRAMPS spectra of  $\text{Ca}(\text{OH})_2$ , malonic acid, and  $\text{KHSO}_4$  along with calculated spectra corresponding to the parameters in Table 1. The chemical shielding parameters in Table 1 have been determined by iterative fitting of the experimental spinning sideband intensities using the simple scaling approach discussed above.  $\text{Ca}(\text{OH})_2$  (Figs. 5a and 5d) and malonic acid (Figs. 5b and 5e) represent examples of quite small  $^1\text{H}$  CSAs which are accessible using MSHOT-3 based CRAMPS under slow-speed spinning conditions (specifically,  $\omega_r/2\pi = 710$  Hz and  $N = 16$ ). In both cases excellent agreement between the experimental spectra and the corresponding optimized simulations is obtained. It is noted, however, that difficulties in separating the two overlapping spinning sideband manifolds for the acidic proton sites in malonic acid by deconvolution may introduce

some uncertainty in the parameters determined for this compound. The two inequivalent protons in  $\text{KHSO}_4$  are characterized by very large  $^1\text{H}$  CSAs spanning a frequency range larger than the range of isotropic  $^1\text{H}$  chemical shifts as demonstrated in Figs. 5c and 5f. In this case, the favorable broadband characteristics of the MSHOT-3 multiple pulse sequence (21) becomes important. The experimental spectrum (Fig. 5c), recorded using  $\omega_r/2\pi = 695$  Hz, appears free of artifacts (apart from an impurity signal at 7.5 ppm) and display identical linewidths of the spinning sidebands throughout the spectrum. This observation is supported by the favorable agreement between the experimental and optimum fitted spinning sideband manifolds (Fig. 5f) representing the chemical shielding parameters for the two sites  $\text{KHSO}_4$  as listed in Table 1.

In conclusion, we have demonstrated that MSHOT-3-based CRAMPS represents a powerful method for determining the values of the principal components of  $^1\text{H}$  shielding tensors when relying on polycrystalline powders. The high-order truncating MSHOT-3 sequence enables high-quality  $^1\text{H}$  CRAMPS spectra with large spectral width, good off-resonance stability, high-order dipolar truncation, and no tilted-axis artifacts to be recorded routinely. Furthermore, as a practically important result, it proves possible to accurately calculate and iteratively fit experimental spectra using standard software for calculation of MAS spectra with the shielding interaction reduced by the scaling factor of the multiple-pulse sequence. In the most demanding cases of small CSAs and strong homonuclear couplings, typical for methylene protons, the homonuclear decoupling provided by a standard

MAS probe in this work proved insufficient. However, even in demanding cases like this, the method appears feasible when using the high  $^1\text{H}$  RF field strengths offered by commercially available dedicated CRAMPS probes. Due to the combined high-order dipolar truncation, large spectral width and high resonance off-set stability, it is envisaged that MSHOT-3-based CRAMPS will find widespread applications also in the determination of  $^{19}\text{F}$  and  $^{31}\text{P}$  CSAs. Studies along these lines are currently being pursued in our laboratory.

### ACKNOWLEDGMENTS

The use of the Varian UNITY-400 spectrometer sponsored by Teknologistyrelsen at the Aarhus Instrument Centre for Solid-State NMR Spectroscopy, University of Aarhus, is acknowledged. This research has been supported by equipment grants from the Danish Natural Science Research Foundation, Carlsbergfondet, Aarhus University Research Foundation, and Ib Henriksens Fond.

### REFERENCES

- U. Haeberlen, "High-Resolution NMR in Solids. Selective Averaging," Academic Press, New York (1976).
- M. Mehring, "Principles of High Resolution NMR of Solids," 2nd ed., Springer, New York (1983).
- J. Herzfeld and A. E. Berger, *J. Chem. Phys.* **73**, 6021 (1980).
- M. M. Maricq and J. S. Waugh, *J. Chem. Phys.* **70**, 3300 (1979).
- U. Haeberlen and J. S. Waugh, *Phys. Rev.* **175**, 453 (1968).
- P. Mansfield, M. J. Orchard, D. C. Stalker, and K. H. B. Richards, *Phys. Rev. B* **7**, 90 (1973).
- W.-K. Rhim, D. D. Elleman, and R. W. Vaughan, *J. Chem. Phys.* **59**, 3740 (1973).
- D. P. Burum and W.-K. Rhim, *J. Chem. Phys.* **71**, 944 (1979).
- D. G. Cory, *J. Magn. Reson.* **94**, 526 (1991).
- B. Schnabel, U. Haubenreisser, G. Scheler, and R. Müller, in "Proceedings, 19th Congress Ampere," p. 441, Heidelberg, 1976.
- R. G. Pembleton, L. M. Ryan, and B. C. Gerstein, *Rev. Sci. Instrum.* **48**, 1286 (1977).
- B. C. Gerstein, C. Chow, R. G. Pembleton, and R. C. Wilson, *J. Phys. Chem.* **81**, 565 (1977).
- L. M. Ryan, R. E. Taylor, A. J. Paff, and B. C. Gerstein, *J. Chem. Phys.* **72**, 508 (1980).
- R. K. Harris, P. Jackson, L. H. Merwin, B. J. Say, and G. Hägele, *J. Chem. Soc. Faraday Trans. 1* **84**, 3639 (1988).
- R. K. Harris, P. Jackson, and G. J. Nesbitt, *J. Magn. Reson.* **85**, 294 (1989).
- P. Jackson, *J. Magn. Reson.* **90**, 391 (1990).
- G. E. Maciel, C. E. Bronniman, and B. L. Hawkins, *Adv. Magn. Reson.* **14**, 125 (1990).
- C. E. Bronniman, B. L. Hawkins, M. Zhang, and G. E. Maciel, *Anal. Chem.* **60**, 1743 (1988).
- R. E. Taylor, R. G. Pembleton, L. M. Ryan, and B. C. Gerstein, *J. Chem. Phys.* **71**, 4541 (1979).
- M. Hohwy and N. C. Nielsen, *J. Chem. Phys.* **106**, 7571 (1997).
- M. Hohwy, P. V. Bower, H. J. Jakobsen, and N. C. Nielsen, *Chem. Phys. Lett.* **273**, 297 (1997).
- W.-K. Rhim, A. Pines, and J. S. Waugh, *Phys. Rev. B* **3**, 684 (1971).
- L. Zheng, K. W. Fishbein, R. G. Griffin, and J. Herzfeld, *J. Am. Chem. Soc.* **115**, 6254 (1993).
- L. B. Schreiber and R. W. Vaughan, *Chem. Phys. Lett.* **28**, 586 (1974).
- S. F. Sagnowski, S. Aravamudhan, and U. Haeberlen, *J. Magn. Reson.* **28**, 271 (1977).